COBEM 2023 27TH INTERNATIONAL CONGRESS OF MECHANICAL ENGENEERING

ABCM Brazilian Society of Mechanical Sciences and Engineering
27th ABCM International Congress of Mechanical Engineering
December 04-08, 2023, Florianópolis-SC, Brazil

COBEM-2023-0415
Analysis of Shape Memory Alloy Composites Using Micromechanical Models

Alencar José Bernardino
CEFET/RJ - Centro Federal de Educação Tecnológica Celso Suckow da Fonseca
PPEMM - Programa de Pós-Graduação em Engenharia Mecânica e Tecnologia de Materiais
Av. Maracanã, 229 - Rio de Janeiro, Brazil
alencar.bernardino@cefet-rj.br

Lucas Lisbôa Vignoli
Center for Technology and Applications of Composite Materials, Department of Mechanical Engineering, Universidade Federal do Rio de Janeiro, Macaé, RJ, Brazil
ll.vignoli@mecanica.coppe.ufrj.br

Pedro Manuel Calas Lopes Pacheco
CEFET/RJ - Centro Federal de Educação Tecnológica Celso Suckow da Fonseca
PPEMM - Programa de Pós-Graduação em Engenharia Mecânica e Tecnologia de Materiais
Av. Maracanã, 229 - Rio de Janeiro, Brazil
pedro.pacheco@cefet-rj.br

Marcelo A. Savi
Universidade Federal do Rio de Janeiro
Center for Nonlinear Mechanics, COPPE – Department of Mechanical Engineering
P.O. Box 68.503, 21941-972, Rio de Janeiro, Brazil
savi@mecanica.coppe.ufrj.br

Abstract: *Composite materials have been widely explored over the years due to lightweight, fatigue life, corrosion resistance, high stiffness and strength. Many investigations can be found in the literature to model their macromechanical effective properties using micromechanical approaches. On the other hand, shape memory alloys are relatively recent and have unique capabilities due to solid phase transformation generating shape memory effect and pseudoelastic effects. The use of composite materials with embedded shape memory alloy wires, using both materials together, began to be explored in recent years showing promising mechanical behaviors that can be applied in several areas as biomedical, automation and aerospace applications. In order to evaluate macromechanical behavior of a shape memory alloy composite (SMAC), a novel constitutive model with linear phase transformation kinetics is derived for the SMAC. Finite element analysis is developed for a verification of the proposed analytical model considering a micromechanical unit cell. The unit cell consists of a circular cross-section wire surrounded by a polymeric matrix. Analytical and numerical results for uniaxial loads show good agreements. Stress-strain curves are obtained to evaluate pseudoelastic effect and the related hysteresis loops represent the amount of energy dissipated, which is useful for structural vibration applications. The proposed analytical model can be considered a useful and reliable tool to efficiently design SMAC elements.*

Keywords: Shape memory alloys composites, constitutive models, hybrid composites.

1. INTRODUCTION

Shape memory alloys have been widely studied over the years due to the benefits that their physical characteristics provide and some constitutive models have been already presented (Savi *et al.*, 2005*)*. Among the most widely known characteristics, one can mention the shape memory and pseudoelastic effects. Shape memory effect occurs at low temperatures when the material is subjected to a mechanical load-unload process and present a residual strain that can be eliminated by subsequent thermal load, recovering the original shape. On the other hand, pseudoelasticity, or superelasticity, occurs at high temperatures when a material subjected to a mechanical load process and, after unload, all strain is eliminated, presenting however a hysteretic behavior.

Recently, composite materials with shape memory alloys have been investigated (Bayat *et al.*, 2018; Cohades *et al.*, 2018). These materials combine traditional properties of the composite materials with the shape memory alloys properties, making it possible to create more complex structures composed of embedded SMA wires.

Libied *et al.* (2015) investigated shape memory alloy composites by conducting experimental tests on composite plates built with embedded SMA wires. The authors analyzed the response of the composite plate subjected to tension and compression test, including a pre-strained SMA wire. Vignoli *et al*. (2020) explored the pseudoelasticity in SMA composite braces to evaluate structures under earthquake loads.

The goal of this study is to evaluate the mechanical behavior of a SMA composite. Initially, an SMA constitutive model is introduced in Section 2. Next, the effective constitutive model for the SMA composite is derived in Section 3. A comparison between the proposed approach and simulation using the finite element method is discussed in Section 4. Finally, the main conclusions are summarized in Section 5.

2. SMA CONSTITUTIVE MODEL USING LINEAR PHASE TRANSFORMATION KINETICS

There are several constitutive models available in the literature to describe thermomechanical behavior of SMAs. Paiva & Savi (2006) presented a general overview of the subject. An important class of models is the one with assumed phase transformation kinetics. Brinson (1993) proposed a model assuming cosine functions to describe phase transformation kinetics. Adeodato *et al.* (2002) employed polynomial equations that improved the efficiency of the computational implementation, avoiding iterative processes. A simple approach can use linear phase transformation kinetics. In this regard, consider the following constitutive equation,

$$\sigma_{11}^{f} = \sigma_{11}^{f0} + (E_f \varepsilon_{11}^{f} - E_{f0}\varepsilon_{11}^{f0}) - \varepsilon_R (E_f \beta - E_{f0}\beta_0) \tag{1}$$

where σ_{11}^{f} is the fiber longitudinal stress, ε_{11}^{f} is the fiber longitudinal strain, ε_R is the maximum recoverable strain, β is the martensite volume fraction, $E_f = E_A + \beta(E_M - E_A)$ is the fiber elastic modulus, E_A is the austenite elastic modulus, and E_M is the martensite elastic modulus. Additionally, the index “0” denotes the previous state.

The austenite-martensite transformation starts if $\sigma_{11}^{f} = \sigma_{AMs}$ and finishes when $\sigma_{11}^{f} = \sigma_{AMf}$. During this transformation, the martensite volume fraction is given by

$$\beta = \left(\frac{1-\beta_0}{\sigma_{AMf} - \sigma_{AMs}} \right) \sigma_{11}^{f} + \left(\frac{\beta_0 \sigma_{AMf} - \sigma_{AMs}}{\sigma_{AMf} - \sigma_{AMs}} \right) \tag{2}$$

On the other hand, the critical stresses for start and finish of the reverse transformation are $\sigma_{11}^{f} = \sigma_{MAs}$ and $\sigma_{11}^{f} = \sigma_{MAf}$, respectively, and the martensite volume fraction is defined by

$$\beta = \left(\frac{\beta_0}{\sigma_{MAs} - \sigma_{MAf}} \right) \sigma_{11}^{f} - \left(\frac{\beta_0 \sigma_{MAf}}{\sigma_{MAs} - \sigma_{MAf}} \right) \tag{3}$$

Despite this model was previously developed for 1D cases, the transversal strains have a significant influence on the composite. Considering the uniaxial stress state, where $\sigma_{11}^{f} = \sigma_{AMs}$ is the unique non-null stress component, the symmetry condition implies that the transversal strains, ε_{22}^{f} and ε_{33}^{f}, have the same value. Since ε_{11}^{f} is split into elastic and inelastic (phase transformation), it is expected that ε_{22}^{f} and ε_{33}^{f} also have elastic and inelastic parcels. For the elastic transversal strain, the simple Hook’s law can be directly applied. On the other hand, for the inelastic transversal strain, the volume conservation is assumed. These hypotheses imply that the transversal strains are defined by

$$\varepsilon_{22}^{f} = \varepsilon_{33}^{f} = \left(-\frac{\nu_f}{E_f} \right) \sigma_{11}^{f} - 0.5\varepsilon_R \beta \tag{4}$$

where ν_f if the fiber Poisson’s ratio.

3. SMA COMPOSITE CONSTITUTIVE MODEL

The idealized model for SMAC consists of a single-ply laminate with fibers arranged unidirectionally parallel to x_1. The presented model consists of a composite material composed of a SMA fiber embedded in a linear epoxy resin matrix. Figure 1 shows a structure as a whole, on the left side, and the micromechanical unit cell on the right side. The coordinate system is also showed.

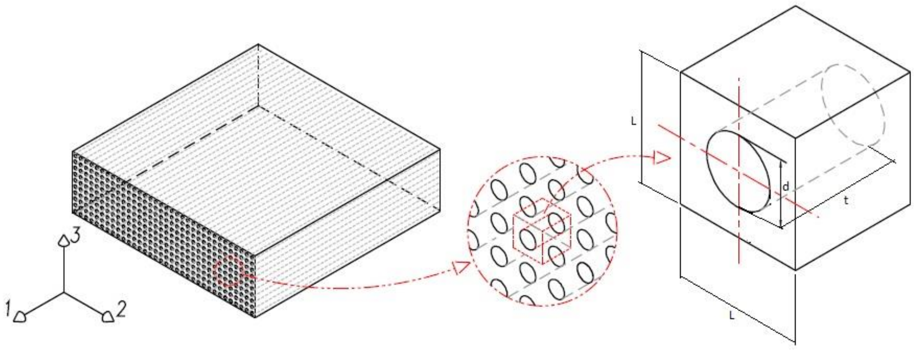

Figure 1: SMA-resin epoxy composite unit cell schematic model for micromechanics analyses.

Considering the longitudinal load, fiber and matrix are in parallel association. Hence, the equilibrium requirement and the geometrical compatibility are defined by

$$\langle \sigma_{11} \rangle = \sigma_{11}^{f} V_f + \sigma_{11}^{m}(1 - V_f) \tag{5}$$

$$\langle \varepsilon_{11} \rangle = \varepsilon_{11}^{f} = \varepsilon_{11}^{m} \tag{6}$$

where $\langle \sigma_{11} \rangle$ is the composite longitudinal stress, σ_{11}^{m} is the matrix longitudinal stress, $\langle \varepsilon_{11} \rangle$ is the composite longitudinal strain, ε_{11}^{m} is the matrix longitudinal strain, and V_f is the SMA fiber volume fraction.

The SMA fiber constitutive model is presented in Eq. (1), while the matrix linear-elastic constitutive equation is

$$\sigma_{11}^{m} = E_m \varepsilon_{11}^{m} \tag{7}$$

where E_m is the matrix longitudinal elastic modulus.

Manipulating these equations, the SMAC constitutive model is defined by

$$\langle \sigma_{11} \rangle = [E_f V_f + E_m(1 - V_f)]\langle \varepsilon_{11} \rangle - \varepsilon_R E_f \beta V_f + \langle \sigma_{11}^{0} \rangle \tag{8}$$

where

$$\langle \sigma_{11}^{0} \rangle = (\sigma_{11}^{f0} - E_{f0}\varepsilon_{11}^{f0} - \varepsilon_R E_{f0}\beta_0)V_f \tag{9}$$

To complete the model derivation, it is desirable to rewrite the equations of the phase transformation kinetics using composite stress, $\langle \sigma_{11} \rangle$. For the forward transformation, the following equation is obtained

$$\beta = \left(\frac{1 - \beta_0}{\langle \sigma_{11}^{AMf} \rangle - \langle \sigma_{11}^{AMs} \rangle} \right) \langle \sigma_{11} \rangle + \left(\frac{\beta_0 \langle \sigma_{11}^{AMf} \rangle - \langle \sigma_{11}^{AMs} \rangle}{\langle \sigma_{11}^{AMf} \rangle - \langle \sigma_{11}^{AMs} \rangle} \right) \tag{10}$$

And the reverse transformation is modeled by

$$\beta = \left(\frac{\beta_0}{\langle \sigma_{11}^{MAs} \rangle - \langle \sigma_{11}^{MAf} \rangle} \right) \langle \sigma_{11} \rangle - \left(\frac{\beta_0 \langle \sigma_{11}^{MAf} \rangle}{\langle \sigma_{11}^{MAs} \rangle - \langle \sigma_{11}^{MAf} \rangle} \right) \tag{11}$$

where $\langle \sigma_{11}^{AMs} \rangle$ is the stress for forward transformation start, $\langle \sigma_{11}^{AMf} \rangle$ is the stress for forward transformation finish, $\langle \sigma_{11}^{MAs} \rangle$ is the stress for reverse transformation start, and $\langle \sigma_{11}^{MAf} \rangle$ is the stress for reverse transformation finish. These critical stresses are derived using the constitutive relations, resulting in the following set of equations

$$\left\langle \sigma_{11}^{AMs} \right\rangle = \sigma_{AMs} V_f + E_m \left(\frac{\sigma_{AMs}}{E_A} \right) (1 - V_f) \tag{12}$$

$$\left\langle \sigma_{11}^{AMf} \right\rangle = \sigma_{AMf} V_f + E_m \left(\frac{\sigma_{AMf}}{E_M} + \varepsilon_R \right) (1 - V_f) \tag{13}$$

$$\left\langle \sigma_{11}^{MAs} \right\rangle = \sigma_{MAs} V_f + E_m \left(\frac{\sigma_{MAs}}{E_M} + \varepsilon_R \right) (1 - V_f) \tag{14}$$

$$\left\langle \sigma_{11}^{MAf} \right\rangle = \sigma_{MAf} V_f + E_m \left(\frac{\sigma_{MAf}}{E_A} \right) (1 - V_f) \tag{15}$$

Next, the composite transversal strains are evaluated. For the sake of simplicity, just $\langle \varepsilon_{22} \rangle$ is defined because $\langle \varepsilon_{22} \rangle = \langle \varepsilon_{33} \rangle$ due the symmetry condition. Considering the transversal strains, fiber and matrix are in series association, what means that the geometrical compatibility is defined as

$$\langle \varepsilon_{22} \rangle = \varepsilon_{22}^{f} V_f + \varepsilon_{22}^{m} (1 - V_f) \tag{16}$$

Eq. (4) can be used as basis for the fiber transversal strain, ε_{22}^{f}, and the linear elastic matrix behavior can be considered to compute the matrix transversal strain, ε_{22}^{m}, using the matrix Poisson's ration, ν_m. Thus, the following equations are obtained

$$\varepsilon_{22}^{f} = \left(-\frac{\nu_f}{E_f} \right) \left(\frac{\langle \sigma_{11} \rangle - E_m \langle \varepsilon_{11} \rangle (1 - V_f)}{V_f} \right) - 0.5 \varepsilon_R \beta \tag{17}$$

$$\varepsilon_{22}^{m} = -\nu_m \langle \varepsilon_{11} \rangle \tag{18}$$

Replacing Eq.(17) and (18) into Eq.(16), the composite transversal strain is

$$\langle \varepsilon_{22} \rangle = \left[\left(-\frac{\nu_f}{E_f} \right) \left(\frac{\langle \sigma_{11} \rangle - E_m \langle \varepsilon_{11} \rangle (1 - V_f)}{V_f} \right) - 0.5 \varepsilon_R \beta \right] V_f - \nu_m \langle \varepsilon_{11} \rangle (1 - V_f) \tag{19}$$

4. RESULTS AND DISCUSSION

This section presents results of the proposed model, establishing a comparison with finite element (FE) simulations, allowing a verification of the new approach. The SMA properties are listed in Table 1, and an epoxy matrix with $E_m = 3.5$GPa and $\nu_m = 0.35$ are considered. Additionally, SMA fiber volume fractions, V_f, of 30%, 50% and 70% were selected in order to evaluate a large variety of SMAC composition. The temperature chosen was 303K.

Table1: SMA constitutive properties according to experimental tests for temperature equal to 303K (Adeodato *et al.*, 2022)

ε_R	E_A [GPa]	E_M [GPa]	$\nu_f = \nu_M = \nu_A$
0.06	33.2	22.1	0.3
σ_{AMs} [MPa]	σ_{AMf} [MPa]	σ_{MAs} [MPa]	σ_{MAf} [MPa]
378.5	402.2	114.2	76.1

A finite element model is developed using the commercial software Ansys. A different constitutive model is employed to describe the SMA thermomechanical behavior (Auricchio *et al.*, 1997), while a linear and elastic matrix is adopted. The unit cell geometry is represented in Figure 2 with the converged mesh for the three selected SMA volume fraction. The interface between fiber and matrix is assumed to be perfectly bonded and the contact pair elements CONTA174 and TARGE170 are adopted combined with the MPC formulation. The periodic boundary condition is imposed to assure the symmetry of the unit cell (Vignoli *et al.* 2022). The SMA fiber has a constant diameter of 1.0mm. Additionally, the unit cell has a thickness of 0.01mm and a transversal section with a width x height of 1.61mm x 1.61mm for V_f = 30%, 1.25mm × 1.25mm for V_f = 50% and 1.05mm x 1.05mm for V_f = 70%.

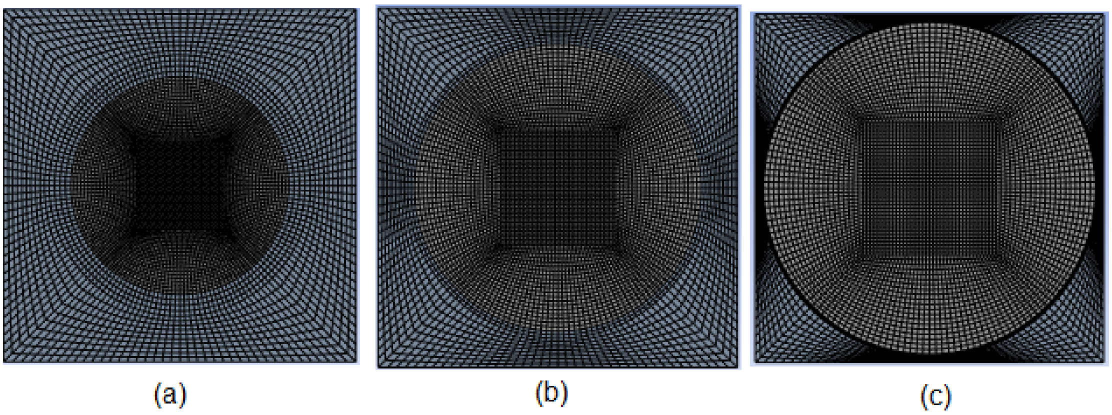

Figure 2: Unit cell for the finite element simulation for volume fractions: (a) V_f = 30%, (b) V_f = 50% and (c) V_f = 70%

The proposed model considers a uniaxial stress state that is represented on the FE unit cell by considering that the load is split into multiple substeps with imposed displacements to keep the periodic boundary condition symmetry. Results of stress and strain components through time for both modeling approaches in the three volume fraction composition are represented in Figure 3. The volume fraction of martensite evolution is presented in Figure 4. It is noticeable a good agreement between both models.

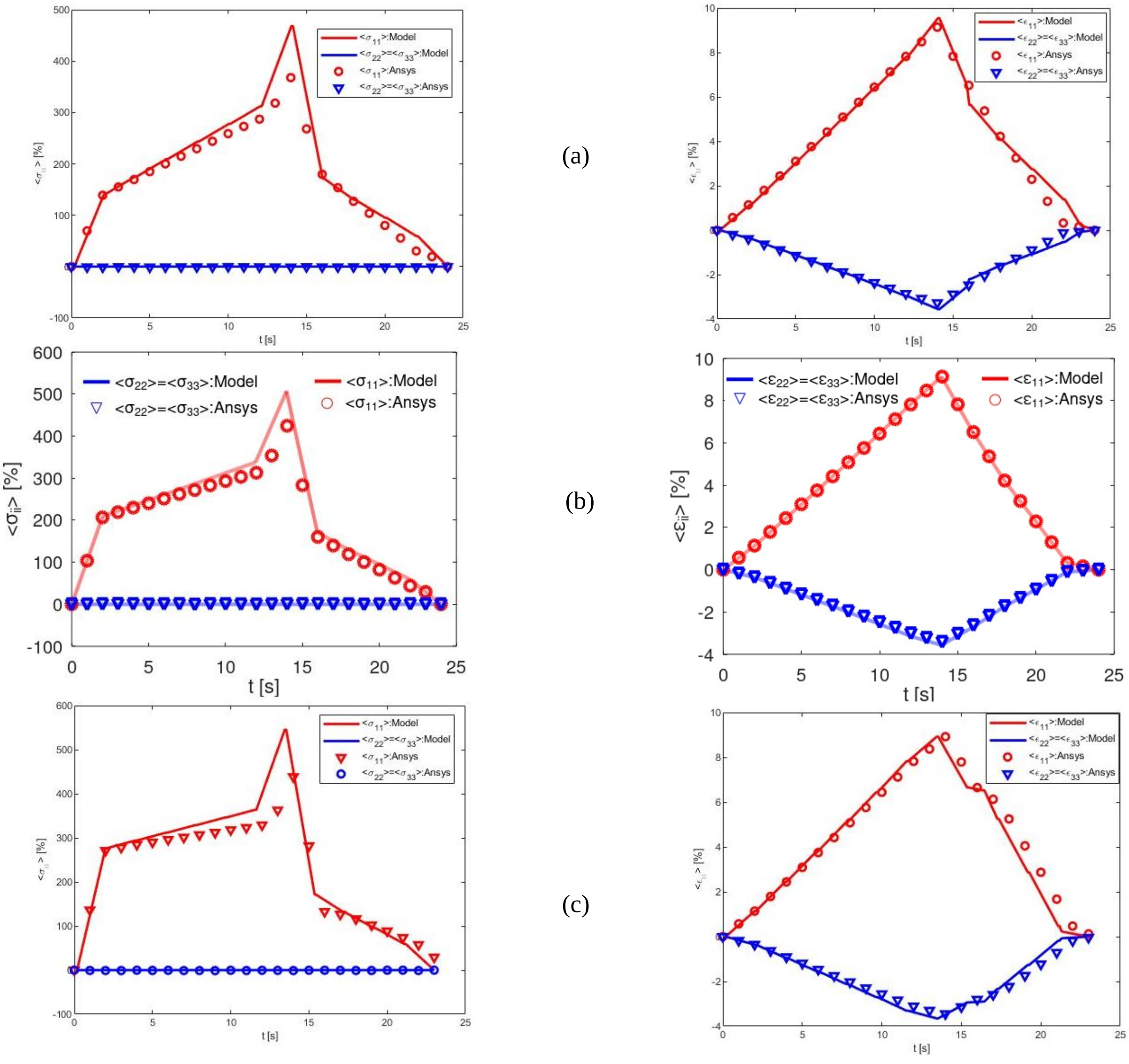

Figure 3: Comparison between the time history of the stress and strain components obtained from the proposed model and the finite element model: (a) V_f = 30%, (b) V_f = 50% and (c) V_f = 70%.

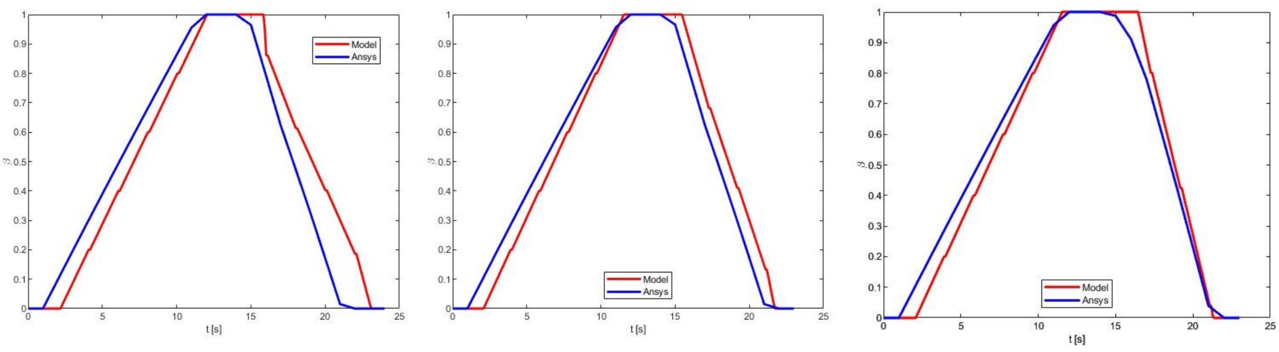

(a) (b) (c)

Figure 4: Comparison between the time history of the volume fraction of martensite obtained from the proposed model and the finite element model: (a) V_f = 30%, (b) V_f = 50% and (c) V_f = 70%.

A comparison between longitudinal stress-strain curves is presented in Figure 5. A good agreement is observed except for a small difference for higher longitudinal strains, which can be explained by the use of different constitutive models. The longitudinal and transversal strains are presented in Figure 6, indicating that volume conservation assumption during the phase transformation is a simple and valid hypothesis.

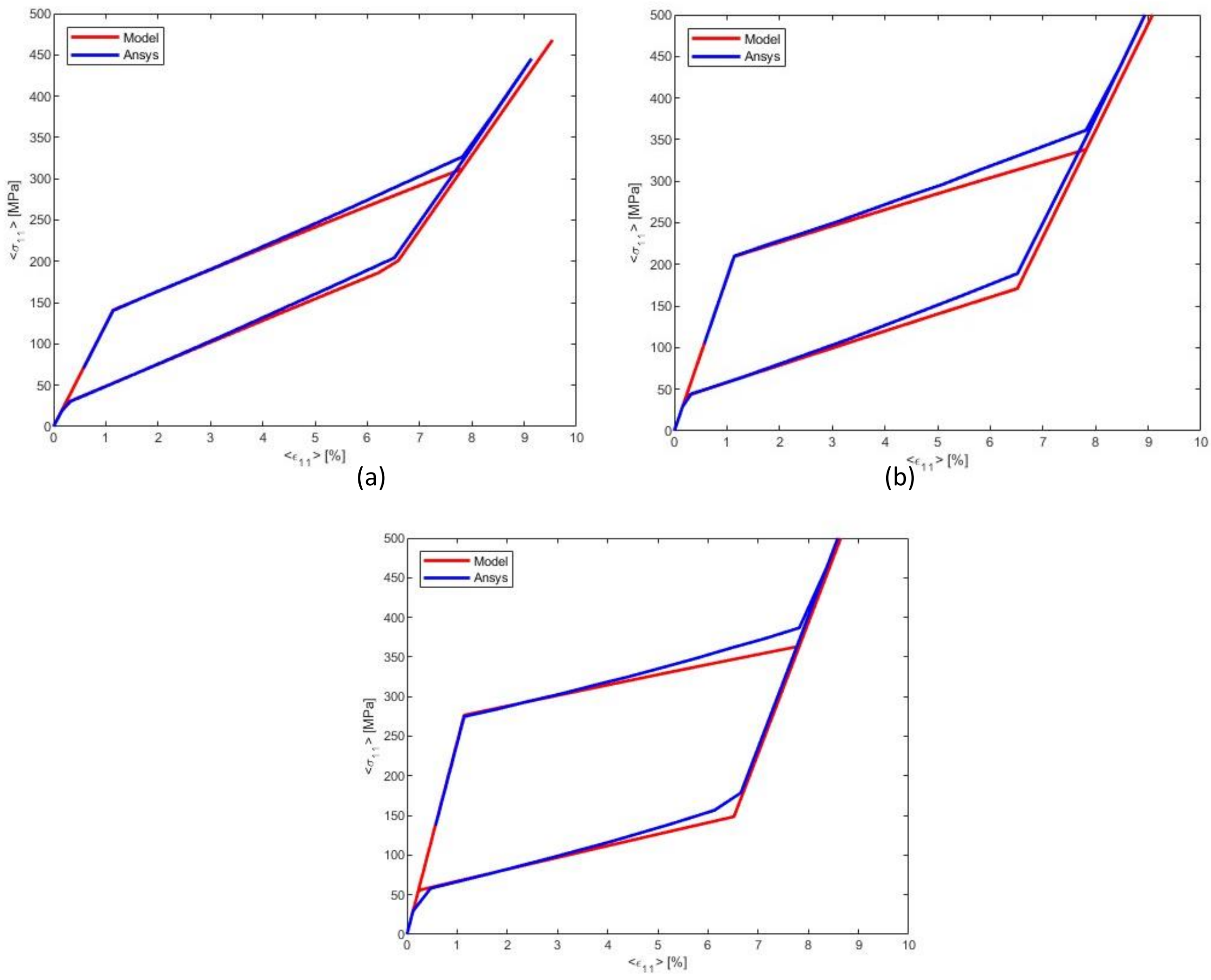

(a) (b)

(c)

Figure 5: Comparison between longitudinal stress-strain curves obtained from the proposed model and the finite element model: (a) V_f = 30%, (b) V_f = 50% and (c) V_f = 70%

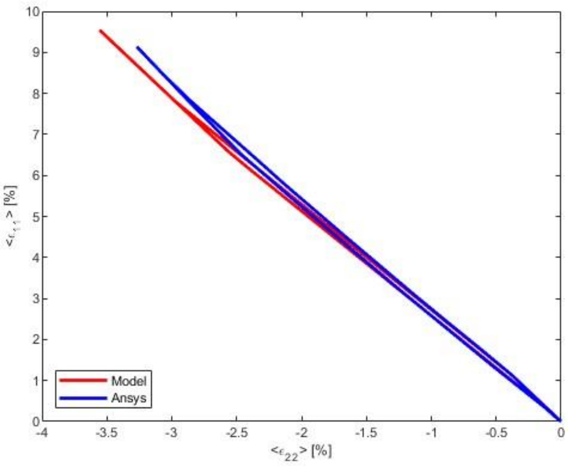

(a)

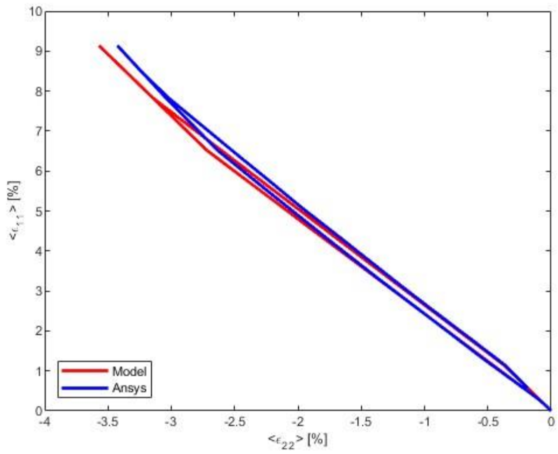

(b)

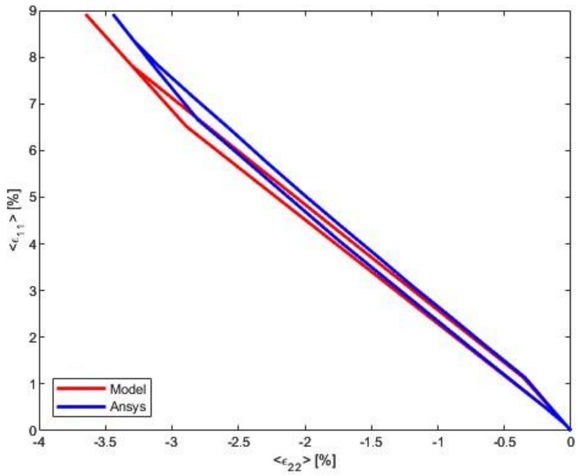

(c)

Figure 6: Comparison between longitudinal and transversal strains obtained from the proposed model and the finite element model: (a) V_f = 30%, (b) V_f = 50% and (c) V_f = 70%

The variation in the effective modulus of elasticity of the hybrid composite can be observed when comparing the stress-strain behavior of the three volume fractions discussed with the homogeneous shape memory alloy wire (V_f = 100%), as showed in Figure 7. As the volume fraction of SMA wires increases, the slopes of the straight lines representing their austenite and martensite phases increase, indicating an increase in the stiffness of the composite. For higher volume fraction compositions, the influence of the matrix elasticity modulus becomes smaller, which indicates a trend of approximation between the composite elasticity and the shape memory alloy moduli.

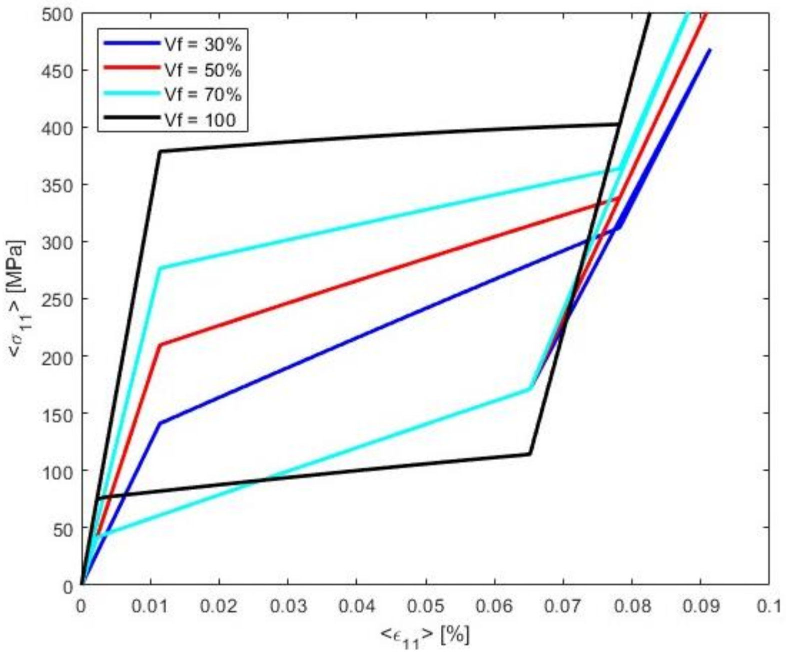

Figure 7: Comparison between stress-strain behavior for the composite volume fractions and the SMA wire.

5. CONCLUSIONS

Shape memory alloy composites (SMACs) have interesting capabilities, such as the possibility of adjusting parameters such as stiffness and energy dissipation produced by hysteretic behavior through changing the volume fraction of the SMA. There are several applications such as reducing vibrations of equipments or structures subjected to earthquakes. Nevertheless, the design of SMAC presents several challenges associated with the involved nonlinearities and the use of numerical models based on the finite element method requires a large amount of computational processing. The goal of this research is to show the effectiveness of a novel analytical model with linear phase transformation kinetics to describe the thermomechanical behavior of an SMAC. Results considering three different shape memory alloy volume fractions are analyzed showing that the proposed methodology is in close agreement with finite element simulations to describe pseudoelasticity. The transversal strain is also evaluated using the volume conservation assumption for the phase transformation strain component and the analytical estimations are also in agreement with FE simulations. The proposed analytical model can be considered a useful and reliable tool for the design SMAC elements.

6. ACKNOWLEDGEMENTS

The authors would like to acknowledge the support of the Brazilian Research Agencies CNPq, CAPES and FAPERJ.

7. REFERENCES

Adeodato, A., Vignoli, L. L., Paiva, A., Monteiro, L. L.S., Pacheco, P. M.C.L., Savi, M. A. “A Shape Memory Alloy Constitutive Model with Polynomial Phase Transformation Kinetics”. Shape Memory and Superelasticity, pag. 277-294. 2022.

Auricchio, F., Sacco, E. “A One-Dimensional Model for Superelastic Shape-Memory Alloys with Different Elastic Properties Between Austenite and Martensite”. Internal Journal Non-Linear Mechanics. 1997

Brinson, L. C. One-dimensional constitutive behavior of shape memory alloys: thermomechanical derivation with non-constant material functions and redefined martensite internal variable. Journal of intelligent material systems and structures, v. 4, n. 2, p. 229-242, 1993

Bayat, Y., Ekhteraeitoussi, H. “A non linear study on structural damping of SMA hybrid composite beam”. Thin Walled Structures. pp. 18-28. 2018.

Cohades A., Michaud, V. “Shape Memory alloys in fiber reinforced polymer composites”. Advanced Industrial and Engineering Polymer Research”. Vol. 1 p. 66-81. 2018.

Lebied, A., Necib, B., Sahli, M.L., Gelin, J.C., Barrière, T. “Numerical simulations and experimental results of tensile behavior of hybrid composite shape memory alloy wires embedded structures”. International Journal of Advanced Manufacture Technologies. 2015.

Paiva, A., Savi, M. A. “An overview of constitutive models for shape memory alloys”. Mathematical Problems in Engineering, volume 2006, p. 1-30. 2005.

Vignoli, L.L., Savi, M.A., El-Borgi, S. “Nonlinear dynamics of earthquake-resistant structures using shape memory alloy composites”. Journal of Intelligent Material Systems and Structures, 31, 771-787, 2020.

Vignoli, L.L., Savi, M.A., Pacheco, P. M. C. L., Kalamkarov, A. “A novel micromechanical model based on the rule of mixtures to estimate effective elastic properties of circular fiber composites”. Applied Composite Materials. 2022

8. RESPONSIBILITY NOTICE

The authors are the only responsible for the printed material included in this paper